European Radiology (2018) 28:2700–2707
https://doi.org/10.1007/s00330-017-5190-4

NUCLEAR MEDICINE

Benefit of ^{18}F-fluorocholine PET imaging in parathyroid surgery

G. F. Huber[1] · M. Hüllner[2] · C. Schmid[3] · A. Brunner[3] · B. Sah[2,4] · D. Vetter[5] · P. A. Kaufmann[2] · G. K. von Schulthess[2]

Received: 15 August 2017 / Revised: 8 November 2017 / Accepted: 9 November 2017 / Published online: 25 January 2018

Abstract

Objectives To assess the additional diagnostic value of ^{18}F-fluorocholine PET imaging in preoperative localization of pathologic parathyroid glands in clinically manifest hyperparathyroidism in case of negative or conflicting ultrasound and scintigraphy results.

Methods A retrospective, single-institution study of 26 patients diagnosed with hyperparathyroidism. In cases where ultrasound and scintigraphy failed to detect the location of an adenoma in order to allow a focused surgical approach, an additional ^{18}F-fluorocholine PET scan was performed and its results were compared with the intraoperative findings.

Results A total of 26 patients underwent ^{18}F-fluorocholine PET/CT ($n = 11$) or PET/MRI ($n = 15$). Adenomas were detected in 25 patients (96.2%). All patients underwent surgery, and the location predicted by PET hybrid imaging was confirmed intraoperatively by frozen section and adequate parathyroid hormone drop after removal. None of the patients needed revision surgery during follow-up.

Conclusions These results demonstrate that ^{18}F-fluorocholine PET imaging is a highly accurate method to detect parathyroid adenomas even in case of previous localization failure by other imaging examinations.

Key Points

- *With ^{18}F-fluorocholine PET imaging, parathyroid adenomas could be detected in 96.2%.*
- *^{18}F-fluorocholine imaging is a highly accurate method to detect parathyroid adenomas.*
- *We encourage its use, where ultrasound fails to detect an adenoma.*

Keywords Hyperparathyroidism · Choline · PET/CT · PET/MR · Minimally invasive surgical procedures

G. F. Huber and M. Hüllner shared first authorship and contributed equally to this work

✉ G. F. Huber
gerry.huber@usz.ch

[1] Department of Otorhinolaryngology, Head & Neck Surgery, University Hospital Zurich, Frauenklinikstrasse 24, 8091 Zurich, Switzerland

[2] Department of Nuclear Medicine, University Hospital Zurich, Rämistrasse 100, 8091 Zurich, Switzerland

[3] Department of Endocrinology, Diabetology, University Hospital Zurich, Rämistrasse 100, 8091 Zurich, Switzerland

[4] Department of Diagnostic and Interventional Radiology, University Hospital Zurich, Zurich, Switzerland

[5] Department of General Surgery, University Hospital Zurich, Rämistrasse 100, 8091 Zurich, Switzerland

Introduction

Hyperparathyroidism is a common endocrine disorder, but still occasionally missed, owing to few and/or unspecific symptoms. Once the diagnosis is established, the only efficient and definite therapy is the removal of the affected parathyroid gland(s). Before it was possible to identify the culprit gland by adequate localization aids (e.g. ultrasound, CT, MR imaging, scintigraphy or combinations thereof [1]), surgical exploration of all parathyroid glands used to be the gold standard. This approach had the major disadvantage that the surgical field was much larger and the operating time considerably longer. Furthermore, ectopic and supernumerary glands, occurring in approximately 5 to 12% in anatomical series [2], prevented surgical success

in some cases (e.g. the famous mariner, Captain Charles Martell [3]). With the improvement of high-quality neck ultrasound, scintigraphy [including different single photon emission computed tomography (SPECT) techniques such as dual-isotope subtraction SPECT, dual-time point SPECT and SPECT/CT] and, more recently, dynamic contrast-enhanced (so-called "4D") CT [4] or MRI, the surgical procedure became site-directed to the gland of interest (focused surgery). By predicting the location of the affected gland at least to the correct side, minimally invasive incisions and minimally invasive video-assisted parathyroid (MIVAP) surgery became possible (Fig. 1). Despite various combinations of different methods, the sensitivity for detecting pathologic glands remains variable [5]. In up to 20% of cases, a pathological parathyroid gland can be detected neither by ultrasound nor scintigraphy [6]. Our standard algorithm would then require a perfusion MRI scan to detect the culprit gland by its typical blood flow characteristics, which is, however, limited in small parathyroid adenomas [7, 8]. A further improvement of the detection accuracy of pathologic parathyroid glands with cross-sectional or functional imaging is therefore quite desirable.

Recently, ^{18}F-fluorocholine PET/CT and ^{11}C-choline PET/CT, otherwise used for diagnosing recurrent prostate carcinoma, were found able to identify pathologic parathyroid glands using [9–13]. Choline tracers used in PET are agents which have been found to accumulate not only in prostate cancer metastases, but also in many other tumors as well as in inflammatory tissue. Choline is a physiological component of cell membranes. Choline expression is increased in neoplasms with high membrane turnover, such as parathyroid adenomas. As a result, and to further improve focused parathyroid surgery, we introduced this imaging technique into clinical routine in our institution in November 2013. Here we report on our results with ^{18}F-fluorocholine hybrid PET to localize pathologic parathyroid glands in patients with negative, weak or conflicting location diagnostics by ultrasound and scintigraphy.

Materials and methods

Inclusion criteria

1. Patients diagnosed with hyperparathyroidism by specialists in endocrinology and nephrology, according to current clinical guidelines [14].
2. Patients with negative, discordant or equivocal results of ultrasonography (US) and scintigraphy (dual-isotope subtraction SPECT using I123 and Tc-99m-tetrofosmin), in whom it therefore was not possible to unambiguously* locate the pathologic parathyroid gland(s).

   *We regarded a result as "ambiguous" when either a negative SPECT was paired with a negative or questionable ultrasound finding (intrathyroid, small lesion or non-hypoechogenic ultrasound image) or when the ultrasound showed an adenoma on the opposite side of the SPECT.

   Dual-isotope subtraction SPECT was regarded doubtful when the subtraction showed only faint uptake that could not be clearly interpreted as adenoma(s).

Exclusion criteria

1. Patients with previous surgery for hyperparathyroidism.
2. Patients in whom the location of the pathologic gland discerned by ultrasound and/or scintigraphy was very likely to be accurate.
3. Patients with documented refusal of general consent to participate in retrospective studies.

Methods

– Dual-isotope scintigraphy was performed as SPECT using 25 MBq of I123 and 525 MBq of Tc-99m tetrofosmin. Subtraction of datasets was performed manually using PMOD 3.5 (PMOD technologies GmbH, Zurich, Switzerland).

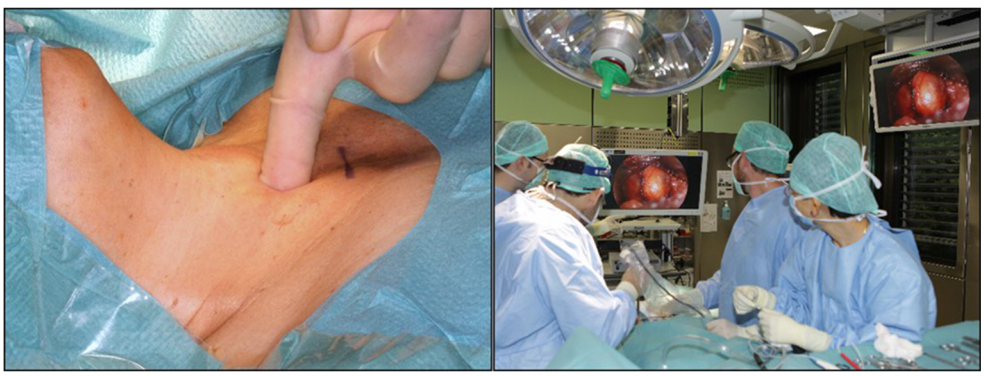

Fig. 1 Minimally invasive surgery: Sufficient incision width of a 2-cm diameter (*left*); swift adenoma detection and mobilization using a 30° optic, called minimally invasive video-assisted parathyroidectomy (MIVAP)

– All PET scans were acquired on time-of-flight scanners (Discovery PET/CT 690 VCT, or Signa PET/MR, GE Healthcare, Waukesha, WI, USA). The PET protocol was almost identical on both systems. The total PET acquisition time was 12–16 min. No fasting and no uptake period were required. The administered standardized dose was 150 MBq of FCh (mean: 151 MBq +/- 16 MBq). The PET scan covered 2–4 bed positions, reaching from the vertex of the skull to the upper abdomen (*Z* axis scanning length of 60 cm). Further detail on image acquisition is given in Tables 1 and 2.

While PET/CT was used in the initial 11 patients, we started using PET/MR with the availability of this technology at our institution. No attempt is made in this study to analyze advantages of one of these hybrid techniques over the other. The interest in the analysis presented is on the PET detection rate. The change from PET/CT to PET/MR has been motivated by the fact that MRI has been preferred over CT in benign head and neck pathology since the 1980s [1].

The primary goal of our study was to determine the methods' success rate in identifying the pathologic gland(s) in patients where the two conventional methods failed to do so. The reference standard for the correct location of an adenoma was based on the results of surgical exploration, confirmed by frozen section and intraoperative drop in parathyroid hormone [PTH] serum concentration by at least 50% 10 min after adenoma removal. Incidental findings of FCh-PET and postoperative success rates were also assessed. Neither the accuracy of ultrasound and scintigraphy were calculated, as the patient cohort was a negative selection, owing to the study design. Sensitivities, specificities and positive predictive values for dual-isotope Tc-99m–tetrofosmin/Tc-99m-sestamibi and I-123 sodium iodide SPECT have been reported before (also by our group) [5, 6, 15].

Results

Between November 2013 and February 2017 (40 months), 26 patients met the inclusion criteria mentioned above (20 females, 76.9%, and 6 males, 23.1%, ratio: 3.3:1) and were included in the study. Median age was 60 years (range 24–83). Twenty-four patients (92.3%) had been diagnosed with primary hyperparathyroidism (PHPT), one (3.85%) with secondary hyperparathyroidism (SHPT) and one (3.85%) with HPT in the context of MEN1. In all patients, the serum PTH was measured preoperatively, with a median of 110.8 ng/l (range: 54.9–257.6 ng/l, reference range: 15–65 ng/l). The corrected preoperative serum calcium concentration ranged from 2.51 to 3.03 mmol/l (median: 2.66 mmol/l).

Table 1 Acquisition parameters for PET/CT imaging

Acquisition parameters for PET/CT imaging	
Parameter	
CT	
Tube voltage	120 kV (peak)
Reference tube current	12.35 mA/slice
Automated dose modulation range	15–80 mAs/slice
Collimation	64 × 0.625 mm
Pitch	0.948:1
Rotation time	0.5 s
Rotation speed	39.37 mm/rotation
Coverage speed	78.75 mm/s
FOV	50 cm
Noise index	20
Reconstruction algorithm	Iterative (ASIR, GE Healthcare)
Soft-tissue images (non-overlapping)	
Kernel	Medium smooth convolution
Window center/width	40/400 HU
Slice thickness	1.25 mm
Isotropic pixel size	0.625 mm
Matrix	512 × 512 pixels
FOV	50 cm
Lung window images (non-overlapping)	
Kernel	Sharp convolution
Window center/width	-600/1200 HU
Slice thickness	1.25 mm
Isotropic pixel size	0.625 mm
Matrix	512 × 512 pixels
FOV	30–35 cm, depending on chest size
PET (3D mode)	
Scan duration	3 min/bed position
Bed positions	3–4, depending on patient size
Axial FOV	153 mm
Emission data correction	Randoms, dead time, scatter, attenuation
Attenuation-corrected images	
Reconstruction algorithm	Iterative (3D TOF OSEM, GE Healthcare)
Reconstruction parameters	3 iterations, 18 subsets
Matrix size	256 × 256 pixels

Notes: AsIR: Adaptive statistical iterative reconstruction, FOV: field of view, HU: Hounsfield unit, OSEM: ordered subset estimation maximization, PET/CT: positron emission tomography/computed tomography, TOF: time of flight

Ultrasound In eight patients (30.8%), no adenoma could be found. In 18 (69.2%), a lesion suspicious for an adenoma was described; nine of them predicted the correct side (50%).

Table 2 Acquisition parameters for PET/MR imaging

Acquisition parameters for PET/MR imaging	
Parameter	
MR	
T1-weighted LAVA-Flex (axial)	
TR/TE [ms]	4.3/1.3 (OP), 2.6 (IP)
Flip angle	12°
Partial Fourier	0.9%
TI [ms]	N/A
Parallel imaging acceleration factor	2
Slice thickness [mm]	4.0
FOV [cm]	50
Acquisition matrix	288 × 224 pixels
Receiver bandwidth [kHz]	142.86
Acquisition time per body section [s]	18
Body sections per patient	4
Total acquisition time [min]	ca. 2
Coverage	Vertex to upper abdomen
T2-weighted (coronal)	
TR/TE [ms]	6647/120
Flip angle	111°
Partial Fourier	N/A
TI [ms]	N/A
Parallel imaging acceleration factor	1
Slice thickness [mm]	5
FOV [cm]	48
Acquisition matrix	288 × 224 pixels
Receiver bandwidth [kHz]	90.91
Acquisition time per body section [s]	60
Body sections per patient	2
Total acquisition time [min]	ca. 2
Coverage	Vertex to upper abdomen
T1-weighted FSE (axial)	
TR/TE [ms]	8.1/2.1
Flip angle	15°
Partial Fourier	N/A
TI [ms]	N/A
Parallel imaging acceleration factor	2Phase/1slice
Slice thickness [mm]	4.0
FOV [cm]	24
Acquisition matrix	320 × 256 pixels
Receiver bandwidth [kHz]	83.33
Acquisition time per body section [s]	N/A
Body sections per patient	N/A
Total acquisition time [min]	0:56
Coverage	Neck
T2-weighted IDEAL fat sat (axial)	
TR/TE [ms]	5414/80
Flip angle	142°
Partial Fourier	N/A
TI [ms]	N/A
Parallel imaging acceleration factor	2
Slice thickness [mm]	4.0
FOV [cm]	24
Acquisition matrix	320 × 256 pixels
Receiver bandwidth [kHz]	83.33
Acquisition time per body section [s]	N/A
Body sections per patient	N/A
Total acquisition time [min]	3:48
Coverage	Neck
T2-weighted STIR (coronal)	
TR/TE [ms]	12387/45
Flip angle	142°
Partial Fourier	N/A
TI [ms]	175
Parallel imaging acceleration factor	2
Slice thickness [mm]	3.5
FOV [cm]	26
Acquisition matrix	256 × 192 pixels
Receiver bandwidth [kHz]	50.0
Acquisition time per body section [s]	N/A
Body sections per patient	N/A
Total acquisition time [min]	4:57
Coverage	Neck
PET (3D mode)	
Scan duration	3 min/bed position
Bed positions	2–4, depending on patient size
Axial FOV	246 mm
Emission data correction	Randoms, dead time, scatter, attenuation
Attenuation-corrected images	
Reconstruction algorithm	Iterative (3D TOF OSEM, GE Healthcare)
Reconstruction parameters	2 iterations, 28 subsets
Matrix size	256 × 256 pixels

Notes: FOV: field of view, FSE: fast spin echo, IDEAL: iterative decomposition of water and fat with echo asymmetry and least-squares estimation, IP: in phase, LAVA: liver acquisition with volume acquisition, N/A: not applicable, OP: opposed phase, OSEM: ordered subset estimation maximization, PET/MR: positron emission tomography/magnetic resonance, STIR: short TI inversion recovery, TE: time to echo, TI: inversion time, TOF: time of flight, TR: time of repetition

Scintigraphy In 24 patients (92.3%), no adenoma was detected or was equivocal. In two (7.7%), a location was described but conflicted with ultrasonographic findings (opposite side).

All patients underwent a FCh-PET/CT ($n = 11$) or FCh-PET/MRI ($n = 15$) scan. FCh-PET was negative in one patient (3.85%) only. In 23 patients, a single location was identified (Fig. 2), and in 2 patients, 2 locations (Fig. 3) were identified. In 12 patients (46.2%), FCh uptake was located at the left-sided lower pole of the thyroid gland, adjacent to the trachea, representing the most common location. Other locations included the right lower pole ($n = 11$) and two separate locations ($n = 2$). In 7 patients (26.9%), an adenoma could be localized by ultrasound, scintigraphy and FCh-PET. However, there was either a discrepancy between the two first exams or there was reasonable doubt whether the location predicted by scintigraphy and ultrasound was correct, meaning that the lesion seen on ultrasound was very small (<5 mm), isoechogenic

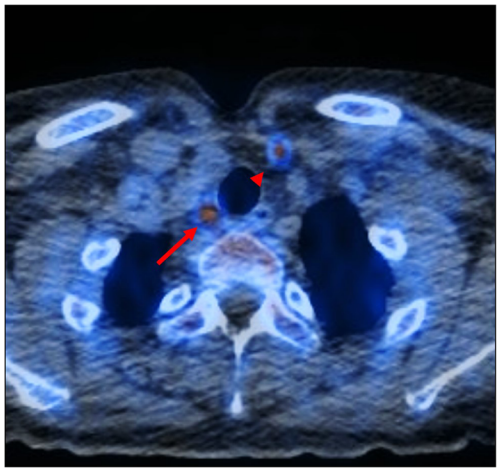

Fig. 3 Patient with bilateral adenomas: right upper mediastinum (*arrow*) and left paratracheal space (*arrowhead*)

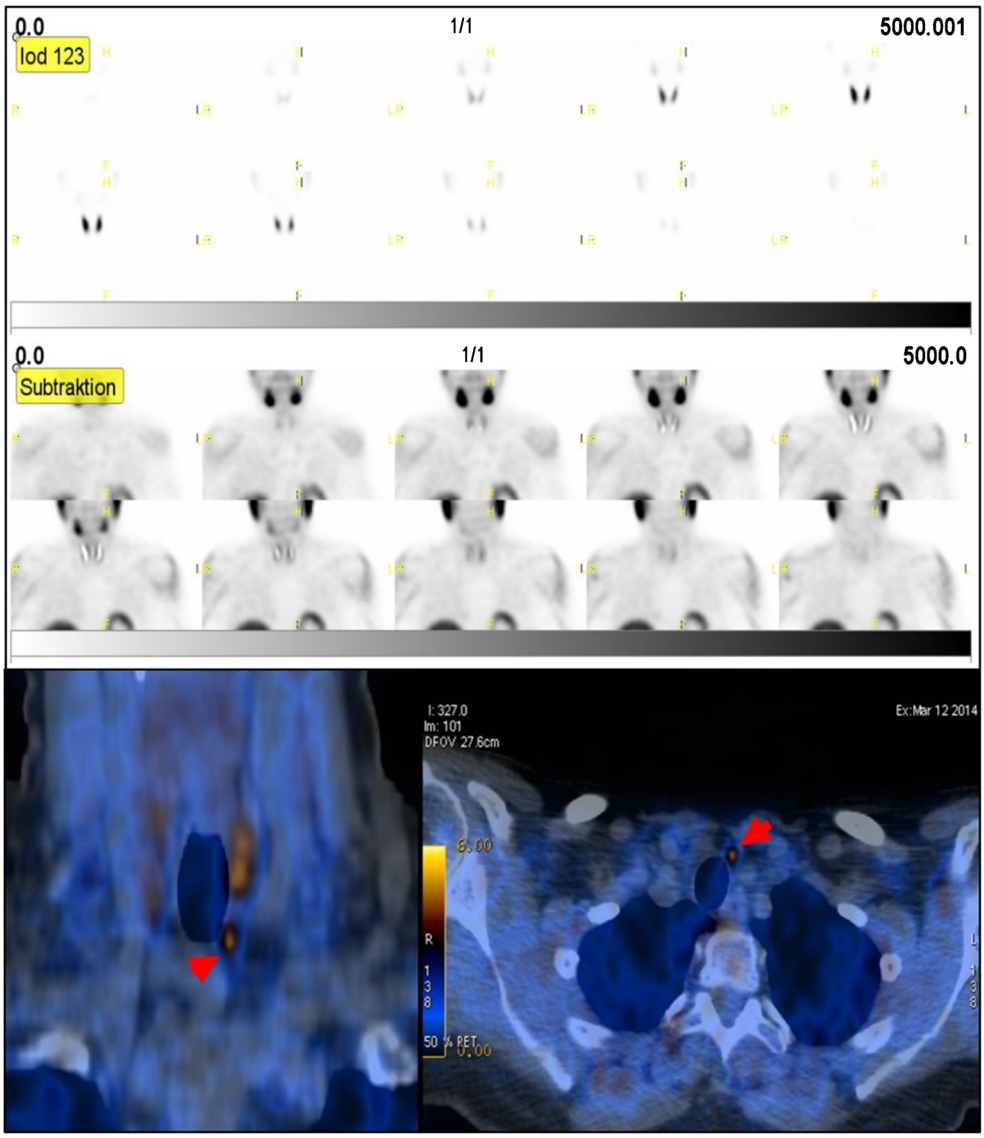

Fig. 2 Negative dual-isotope subtraction SPECT, but positive localization of a culprit gland on FCh-PET/CT. The *upper row* (I123 SPECT) and *middle row* (I123/Tc-99m SPECT subtraction) show a conventional scan that is negative for a parathyroid adenoma. The *lower row* (FCh-PET/CT) shows a FCh-positive adenoma (*red arrow*) at the left lower thyroid pole (coronal view *left*, axial view *right*)

compared with thyroid tissue, ill-defined on ultrasound or not clearly localizable by scintigraphy. In five of those, the location predicted by FCh-PET was identical with both ultrasound and scintigraphy. The two cases identified on scintigraphy, which had conflicting ultrasound findings, were correct on FCh-PET.

All patients were operated upon at our institution. In 12 patients (46.2%), the operation was minimally invasive and video-assisted (MIVAP); in the rest (53.8%); the operation was minimally invasive or open (Kocher incision). Open surgery was planned from the outset if the normal anatomy was distorted by previous surgery ($n = 4$; e.g. after previous thyroidectomy) or if a patient was under platelet aggregation inhibition. An intraoperative conversion to open surgery was done if the intraoperative blood loss was higher than expected ($n = 4$). No complications were documented (permanent recurrent laryngeal nerve palsy, postoperative bleeding, wound infection). Treatment effectiveness was documented by considering frozen section results (confirmed hyperplastic parathyroid tissue) and at least 50% PTH drop 10 min after excision compared to the preoperative value.

In two patients, the intraoperative PTH drop was initially less than the expected 50%, and further exploration revealed a more posteriorly located adenoma (the location predicted by FCh-PET was still correct, the adenoma was just somewhat more posterior than usual; e.g. descended upper adenoma posterior to the recurrent laryngeal nerve). In another 2 patients, the PTH drop was less than 50% 10 min after removal of the pathologic gland, but in the frozen section, there was no doubt that the parathyroid adenoma had been identified and removed completely. In both patients, Ca^{++} levels and PTH levels were within the physiologic range postoperatively. In 19 of 26 patients (73.1%), a follow up of at least 6 months was documented, and in all of them, the serum concentration of PTH and Ca^{++} maintained normal levels. No patient has needed revision surgery so far (median follow-up 17 months; range: 1–37).

By FCh-PET, only in 1 out of 26 patients (3.9%), no parathyroid adenoma was found (sensitivity of 96.2%). The location predicted by FCh-PET was confirmed intraoperatively in all cases where FCh-PET was positive, reverting to a positive predictive value of 100%.

Discussion

Parathyroid surgery used to be a time-consuming procedure where the position of all parathyroid glands had to be explored (four-gland exploration). The experience of the surgeon was and is the main indicator for success. Intraoperative frozen sections and PTH measurement were crucial steps to increase the surgical success rate. With the development of high-resolution ultrasound and other cross-sectional imaging modalities, the success rates further increased to a point where focused approaches became possible and a wide exploration to identify the potential whereabouts of pathological glands was no longer necessary. However, even by a combination of ultrasound and scintigraphy, it is not always possible to locate the gland of interest. In our cohort, ultrasound was falsely positive more often than dual-isotope scintigraphy, which was falsely negative in most patients. False positive results are less commonly achieved with scintigraphy than with ultrasound, because structures that might mimic parathyroid adenomas on ultrasound (e.g. lymph nodes) are consistently negative on scintigraphy [6, 16].

Although FCh-PET has been described for location diagnostics of parathyroid adenomas before [9–13, 17–19], our study represents the first meticulously documented application where only a regionalized PET scan was performed. The axial FOV (Z axis) of 51–82 cm was sufficient to cover all potential parathyroid adenoma locations from the skull base to the diaphragm (actual Z axis coverage depending on patient size; 2–4 bed positions per patient, 15/25 cm axial coverage per bed position with an overlap of 24%).

Compared with the studies of Michaud et al. [20, 21], where a sensitivity of 89% was reported for the detection of parathyroid adenomas, our results were slightly higher (96.2%). However, this may be due to our highly selected cohort and comparably lower number of patients with secondary hyperparathyroidism. Kluijfhout et al. [22] also investigated the benefit of 18F-fluorocholine PET/CT in patients where ultrasound and Tc-99m-sestamibi SPECT/CT failed to detect an abnormal gland. In 4 of 5 patients (80%), the method enabled minimally invasive parathyroidectomy. In the study of Orevi et al. [23], the detection rate of parathyroid adenoma by 11C-choline PET/CT was higher as with Tc-99m sestamibi scintigraphy, but sensitivity was not calculated due to lack of complete surgical validation. A similar sensitivity of 18F-fluorocholine PET as in our study was reported by Lezaic et al. [24] (92%).

Since our study analyzed the diagnostic performance of FCh-PET in patients where SPECT failed to detect a culprit lesion, the diagnostic accuracy of other scintigraphic methods reported in the literature is not directly comparable with the results of our study, owing to a different selection of patients. A prospective direct comparison of different scintigraphic methods, including FCh-PET, in a larger general population of patients with pHPT is desired. To date, mainly retrospective studies or studies with mixed populations of pHPT and sHPT exist [21–23]. One prospective study in pHPT patients, including 24 patients, reported higher sensitivity and equal specificity of FCh-PET compared to different SPECT/CT techniques [24]. We acknowledge that our study used SPECT and not SPECT/CT. SPECT/CT might have helped in some of the ambiguous cases. While most studies on this topic report SPECT/CT to be somewhat superior to SPECT for

localizing parathyroid adenomas, other authors could not show an advantage of SPECT/CT over SPECT and suggested to refrain from the additional radiation exposure. However, SPECT/CT is currently considered the standard of care [25–27].

In our study, we had no false positive results. Potential false positives on FCh-PET would include, but are not limited to, thyroid nodules, inflammatory lymph nodes, and nodal metastases. Due to the high positive predictive value of FCh-PET, we could demonstrate that even in unclear cases, focused surgery with a swift detection of the pathologic gland is feasible. Even though costs for FCh-PET are still reasonably high, the achieved saving of operative time justifies its application, not only if ultrasound and scintigraphy fail to detect the pathologic gland.

Radiation exposure Patients with hyperparathyroidism are often young and they are suffering from a benign disease. Therefore, they have a comparably high life expectancy. Reducing the effective radiation dose in these patients is even more appreciable than in oncologic patients. Compared to dual-isotope scintigraphy with 10 to 15 mSv and dual-phase scintigraphy with 3 to 8 mSv [28], FCh-PET/MR using 150 MBq yields an estimated effective dose of approximately 2.5 mSv [29]. This aspect has already been discussed by van Raalte et al. [30] in their case series.

Cost-effectiveness The expenses in Switzerland for scintigraphy are approximately 1700 CHF (Swiss Francs; ~1660 US$). In case of negative or conflicting results, we would opt for an MRI (800 CHF; ~781 US$). Taken together, the costs are 2500 CHF (~2440 US$). The costs for an FCh-PET are approximately 2600 US$ which is insignificantly more expensive. Moreover, the additional costs are well spent, given the high sensitivity and positive predictive value, allowing a time-saving focused operating technique. One drawback of FCh-PET in HPT patients is still the unavailable reimbursement by most health insurances for this indication.

Summary

FCh-PET was found able to accurately detect parathyroid adenoma(s) in patients with hyperparathyroidism in whom localization by ultrasound and scintigraphy failed, thereby facilitating a swift intraoperative detection by minimally invasive (and video-assisted) techniques. We therefore encourage its use not only in cases where ultrasound and/or scintigraphy are not successful in detecting the location of the adenoma or have led to conflicting results, but also in cases where no gland can be detected by ultrasound. This recommendation is also supported by considerably less radiation exposure from FCh-PET/MR than from conventional scintigraphy used for parathyroid adenoma localization. FCh-PET might become the new standard of care in location diagnostics for parathyroid adenomas, at least if other imaging modalities failed to detect a culprit parathyroid gland.

Funding The authors state that this work has not received any funding.

Compliance with ethical standards FCh-PET in patients with HPT is an approved clinical imaging procedure in our country, and is therefore partly reimbursed by health insurance. Permission for conducting our study was obtained by the ethical committee responsible for our hospital (no. 2016-01616). Due to the retrospective nature of our study, written general informed consent of patients was deemed sufficient by the institutional review board for inclusion into the study. Patients who refused to give signed informed consent were not included into the study. All co-authors mentioned above disclose no potential conflicts of interest.

Guarantor The scientific guarantor of this publication is Gerhard Huber.

Conflict of interest The authors of this manuscript declare no relationships with any companies, whose products or services may be related to the subject matter of the article.

Statistics and biometry No complex statistical methods were necessary for this paper.

Informed consent Written informed consent was obtained from all subjects (patients) in this study.

Ethical approval Institutional review board approval was obtained.

Methodology
- prospective
- observational
- performed at one institution

References

1. von Schulthess GK, Weder W, Goebel N et al (1988) 1.5 T MRI, CT, ultrasonography and scintigraphy in hyperparathyroidism. Eur J Radiol 8:157–164
2. Noussios G, Anagnostis P, Natsis K (2012) Ectopic parathyroid glands and their anatomical, clinical and surgical implications. Exp Clin Endocrinol Diabetes 120:604–610
3. Randolph G (2002) Surgery of the Thyroid and Parathyroid Glands, 1st edn. WB Saunders Company, Philadelphia
4. Suh YJ, Choi JY, Kim SJ et al (2015) Comparison of 4D CT, ultrasonography, and 99mTc sestamibi SPECT/CT in localizing single-gland primary hyperparathyroidism. Otolaryngol Head Neck Surg 152:438–443
5. Krakauer M, Wieslander B, Myschetzky PS et al (2016) A Prospective Comparative Study of Parathyroid Dual-Phase Scintigraphy, Dual-Isotope Subtraction Scintigraphy, 4D-CT, and Ultrasonography in Primary Hyperparathyroidism. Clin Nucl Med 41:93–100
6. Sommerauer M, Graf C, Schäfer N et al (2015) Sensitivity and specificity of Dual-Isotope 99mTc-Tetrofosmin and 123I Sodium Iodide Single Photon Emission Computed Tomography (SPECT) in hyperparathyroidism. PLoS One 10(6):e0129194
7. Nael K, Hur J, Bauer A et al (2015) Dynamic 4D MRI for Characterization of Parathyroid Adenomas: Multiparametric Analysis. AJNR Am J Neuroradiol 36:2147–2152

8. Merchavy S, Luckman J, Guindy M et al (2016) 4D MRI for the Localization of Parathyroid Adenoma: A Novel Method in Evolution. Otolaryngol Head Neck Surg 154:446–448
9. Mapelli P, Busnardo E, Magnani P et al (2012) Incidental finding of parathyroid adenoma with 11C-choline PET/CT. Clin Nucl Med 37:593–595
10. Welle CL, Cullen EL, Peller PJ et al (2016) ^{11}C-Choline PET/CT in Recurrent Prostate Cancer and Nonprostatic Neoplastic Processes. Radiographics 36:279–292
11. Quak E, LHeureux S, Reznik Y et al (2013) F18-Choline, a novel PET tracer for parathyroid adenoma? J Clin Endocrinol Metab 98: 3111–3112
12. Hodolic M, Huchet V, Balogova S et al (2014) Incidental uptake of 18Ffluorocholine (FCH) in the head or in the neck of patients with prostate cancer. Radiol Oncol 48:228–234
13. Cazaentre T, Clivaz F, Triponez F (2014) False-positive result in 18Ffluorocholine PET/CT due to incidental and ectopic parathyroid hyperplasia. Clin Nucl Med 39:328–330
14. Wilhelm SM, Wang TS, Ruan DT et al (2016) The American association of endocrine surgeons guidelines for definitive management of primary hyperparathyroidism. JAMA Surg 151(10):959–968
15. Barber B, Moher C, Cote D et al (2016) Comparison of single photon emission CT (SPECT) with SPECT/CT imaging in preoperative localization of parathyroid adenomas: a cost-effectiveness analysis. Head Neck 38 Suppl 1:E2062–5
16. Frank SJ, Goldman-Yassen AE, Koenigsberg T, Libutti SK, Koenigsberg M (2017) Sensitivity of 3-dimensional sonography in preoperative evaluation of parathyroid glands in patients with primary hyperparathyroidism. J Ultrasound Med 36(9):1897–1904
17. Lalire P, Ly S, Dequelte S et al (2017) Incremental Value of 18F-Fluorocholine PET/CT in the Localization of Double Parathyroid Adenomas. Clin Nucl Med 42:218–220
18. Huellner MW, Aberle S, Sah BR et al (2017) Visualization of Parathyroid Hyperplasia Using 18F-Fluorocholine PET/MR in a Patient With Secondary Hyperparathyroidism. Eur J Surg Oncol 43:133–137
19. Vellani C, Hodoic M, Chytiris S et al (2017) Early and Delayed 18F-FCH PET/CT Imaging in Parathyroid Adenomas. Clin Nucl Med 42:143–144
20. Michaud L, Balogova S, Burgess A et al (2015) A pilot comparison of 18F-fluorocholine PET/CT, ultrasonography and 123I/99mTc-sestaMIBI dual-phase dual-isotope scintigraphy in the preoperative localization of hyperfunctioning parathyroid glands in primary or secondary hyperparathyroidism: influence of thyroid anomalies. Medicine (Baltimore) 94(41):e1701
21. Michaud L, Burgess A, Huchet V et al (2014) Is 18F-fluorocholine-positron emission tomography/computerized tomography a new imaging tool for detecting hyperfunctioning parathyroid glands in primary or secondary hyperparathyroidism? J Clin Endocrinol Metab 99:4531–4536
22. Kluijfhout WP, Vorselaars WM, Vriens MR et al (2015) Enabling minimal invasive parathyroidectomy for patients with primary hyperparathyroidism using Tc-99m-sestamibi SPECT-CT, ultrasound and first results of (18)F-fluorocholine PET-CT. Eur J Radiol 84: 1745–1751
23. Orevi M, Freedman N, Mishani E et al (2014) Localization of parathyroid adenoma by ^{11}C-choline PET/CT: preliminary results. Clin Nucl Med 39:1033–1038
24. Lezaic L, Rep S, Sever MJ et al (2014) ^{18}F-Fluorocholine PET/CT for localization of hyperfunctioning parathyroid tissue in primary hyperparathyroidism: a pilot study. Eur J Nucl Med Mol Imaging 41:2083–2089
25. Gayed IW, Kim EE, Broussard WF et al (2005) The value of 99mTc-sestamibi SPECT/CT over conventional SPECT in the evaluation of parathyroid adenomas or hyperplasia. J Nucl Med 46: 248–252
26. Vaz A, Griffiths M (2011) Parathyroid imaging and localization using SPECT/CT: initial results. J Nucl Med Technol 39:195–200
27. Lavely WC, Goetze S, Friedman KP et al (2007) Comparison of SPECT/CT, SPECT, and planar imaging with single- and dual-phase (99m)Tc-sestamibi parathyroid scintigraphy. J Nucl Med 48:1084–1089
28. Greenspan BS, Dillehay G, Intenzo C et al (2012) SNM practice guideline for parathyroid scintigraphy 4.0. J Nucl Med Technol 40: 111–118
29. Giussani A, Janzen T, Uusijärvi-Lizana H et al (2012) A compartmental model for biokinetics and dosimetry of 18F-choline in prostate cancer patients. J Nucl Med 53:985–993
30. van Raalte DH, Vlot MC, Zwijnenburg A et al (2015) F18-Choline PET/CT: a novel tool to localize parathyroid adenoma? Clin Endocrinol 82:910–912